JJMIE

Volume 4, Number 3, June, 2010
ISSN 1995-6665
Pages 412 - 417

Jordan Journal of Mechanical and Industrial Engineering

Simulation and Modeling of Bubble Motion in an Electrolytic Bath of Soderberg Pot

C. Karuppannan, T.Kannadasan

CIT Sandwich Polytechnic College, Coimbatore-641 014, Tamilnadu, India

Abstract:

In Aluminium manufacturing the Soderberg pot is widely used. The study explains about the bubble motion in cryolite liquid in a Soderberg pot anode face using comprehensive VOF multiphase model in FLUENT, under the action of gravitation. The distribution of bubbles introduced under the anodes of an aluminum reduction cell at the initial time has fixed size. 2D simulation results are reported for four cases with different initial conditions for the bubbles, physics and geometries.

Keywords: Bubble analysis; Aluminium manufacturing;numerical simulation;VOF model.

1. Introduction

In aluminium manufacturing, formation of bubbles is a major problem. Soderberg pots are used for the manufacture of aluminium. In Soderberg pot, the bubbles are formed in the interpolar distance and deposited on the anode face due to the thermal and chemical reactions in the electrolytic bath. It reduces the input power and increases the energy consumption and reduces the current efficiency. Reduction in the formation of bubbles will increase the current efficiency of the pot and output of aluminium. From the previous studies, the temperature distribution is clearly studied and proved. It has been reported that formation of bubbles is from the anode surface. Hence, a model of the anode surface is taken for the analysis. Initial distributions of bubbles and diameters of the bubbles are taken at random. Bubbles considered are having a non-zero density and deformable body; therefore having an appropriate mass (depending on the volume), hence providing a more accurate mathematical model. With the aid of comprehensive **Volume Of Fluid** (VOF) model in FLUENT under the action of gravitation, the formed bubbles are coalescence and collapsed. The result is compared with the mathematical model. The above work proves that the bubbles are collapsed with the increase in pressure in the feeding of Alumina. In this we can achieve the result accurately and enhance the current efficiency and quality of Aluminium production.

2. Governing Equations

To solve the given cryolite and bubble phase flow, field employs the conservation equations for mass and momentum for incompressible fluid.

$$\nabla \cdot u \tag{1}$$

$$\frac{\partial(\rho u_j)}{\partial t} + \nabla \cdot \left(\rho u_i u_j\right) = -\nabla p + \rho g_j + \nabla \cdot \mu\{(\nabla \vec{u}) + (\nabla \vec{u})^T\} + F_j; \text{where j = cryolite} \tag{2}$$

Momentum equations are solved for both cryolite and fluid. Continuum surface model (CSF) is used to describe the interfacial surface tension.

$$\frac{\left(\alpha_q^n \rho_q^n - \alpha_q^{n-1} \rho_q^{n-1}\right)}{\Delta t} + \sum_{nof}\left(\rho_q U_{nof}^{n-1} \alpha_{q,nof}^{n-1}\right) = \sum_{p=1}^{2}\left(\dot{m}_{pq} - \dot{m}_{p}\right) \tag{3}$$

Equation (3) represents the VOF model governing equation for the cryolite-bubble phase model, where density and viscosity are defined

$$\rho\_mix = \alpha\_air\, \rho\_air + (1 - \alpha\_air)\, \rho\_cryolite$$

and

$$\mu_{mix} = \alpha_{air}\mu_{air} + (1 - \alpha_{air})\mu_{cryolite}$$

Primary volume fraction will be computed based on

$$\alpha_{cryolite} + \alpha_{air} \tag{4}$$

3. Numerical Solution

Properties of cryolite and bubble used for the analysis are shown in Table 1. Model and meshing are done in GAMBIT.

Table 1 Properties of Cryolite and Bubble

Property	Cryolite	Air (Bubble)
Density	2567 kg/m^3	1.225 kg/m^3
Viscosity	1.57 cP	0.017894 cP
Surface Tension	0.05 N/m	

The model presented in this paper used VOF model (2).

$$\alpha_{air}(x,y,t), \text{volume fraction} = \begin{cases} 0, cell\ filled\ with\ fully\ cryolite \\ 1, cell\ filled\ with\ fully\ air \\ > 0\ and < 1, mixture\ of\ cryolite\ and \end{cases} \tag{5}$$

For interpolation of cryolite-bubble interface cell region, Geometric Reconstruction Scheme is used. The geometric reconstruction scheme represents the interface between fluids using a piecewise-linear approach. When the cell is near the interface between two phases, the geometric reconstruction scheme is used to obtain the face fluxes. It assumes that the interface between two fluids has a linear slope within each cell, and uses this linear shape

for calculation of the advection of fluid through the cell faces. The first step in this reconstruction scheme is calculating the position of the linear interface relative to the center of each partially-filled cell, based on information about the volume fraction and its derivatives in the cell. The second step is calculating the amount of fluid through each face normally using the computed linear interface representation and information about the normal and tangential velocity distribution on the face. The third step is calculating the volume fraction in each cell using the balance of fluxes calculated during the previous step.

Body force weighted scheme for differencing, Explicit scheme for temporal and PISO for pressure velocity coupling is used for solving.

4. Results & Discussions

4.1. Case 1: Coalescence with Gravity: Small Bubble and Big Bubble Below

Domain dimensions are 20 mm x 10 mm surface. Geometry with three fluid zones is modelled viz., Cryolite, Bigger bubble and smaller bubble. Bubble walls are marked as interior. Results at time steps 0s, 0.03s, 0.033s, 0.036s are shown.

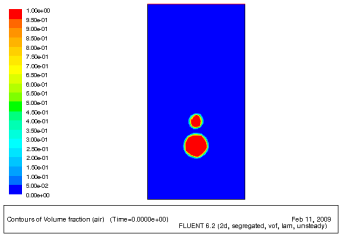

a) initial configuration at t = 0s

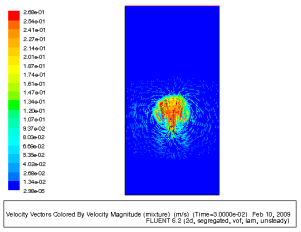

b) t = 0.03s

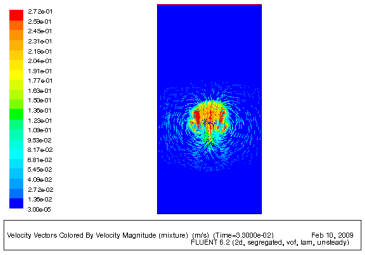

t = 0.033s

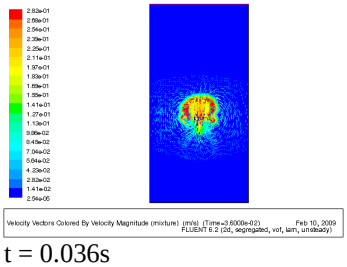

t = 0.036s

Figure 4-1. Coalescence of two rigid circular bubbles. The contours of the bubbles as well as the fluid velocity vectors are shown.

The above results show that the bubbles move through the cryolite medium towards upwards under the action of buoyancy since the system is in the gravitational field. The bubbles having a lower density than the surrounding liquid medium displace the liquid, volume equivalent to their own volume and this displaced liquid wants to push the bubble upwards so as to occupy its volume. This is in accordance with the Archimedes' principle. Also, bigger bubble moves faster than the smaller bubble due to different buoyant force exerted depending on their volume. This phenomenon therefore contributes to the different velocities of the bubbles.

The coalescence occurs already at time 0.03 seconds as opposed to the results depicted in the paper (3). This can be just due to different densities of the continuous fluid (in our case cryolite) which causes different speeds being attained by the bubble, hence decreasing the time to coalesce. The animation also shows the bigger bubble attaining a protruded shape in the beginning owing to being in the wake of the smaller bubble due to which it is in a low pressure region and gets specially pulled into the smaller bubble before coalescence occurs. These findings can be verified by the paper (3).

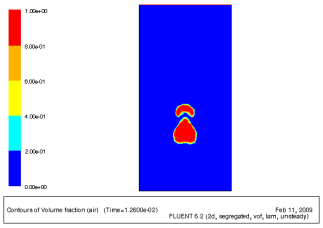

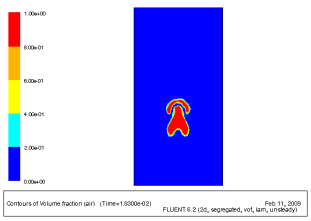

Figure 4-2. Typical C-shape morphology attained by the smaller bubble. Protruding shape of the bigger bubble, caught in the wake of the rising smaller bubble

4.2. Case 2: Surface Tension Effect: Single Elliptical Bubble with Different Surface Tension Values of the Fluid

Domain dimensions are 20 mm x 12 mm. Normal bubble rising problem with constant surface tension specification (0.05 N/m). Results at time steps t = 0.1s, t = 0.1s, t = 0.05s are shown.

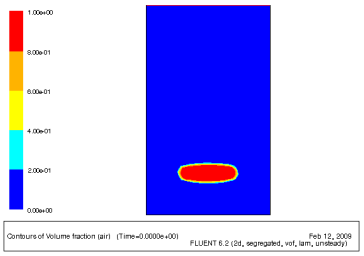

a) initial configuration, t=0s

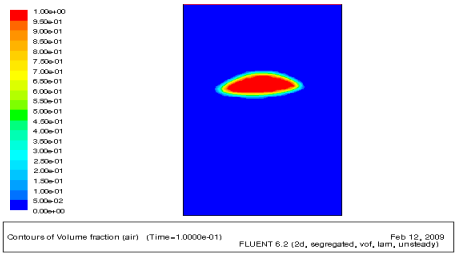

b) bubble configuration at t = 0.1s, α_s = 0.05 N/m

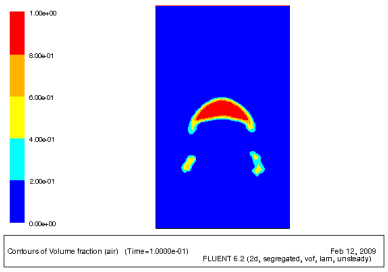

c) t = 0.1s, α_s = 0.005 N/m

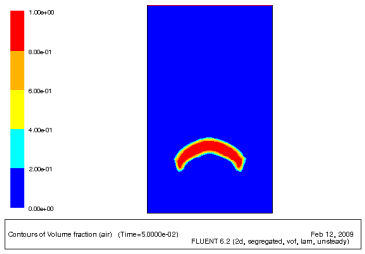

d) time 0.05s, α_s = 0.0005 N/m

Figure 4-3. Influence of the surface tension coefficient α_s

The above results match with the results of the publication qualitatively, although the more intricate details like bubble break-up owing to lower surface tension (figure 2.1(c)) have not been captured in the paper. Besides, the C-shape morphology attained due to the low pressure region in the wake of the rising bubble has been captured much better in the FLUENT simulation. The velocity vector plots overlaid on the bubble images for the four situations explain these phenomena.

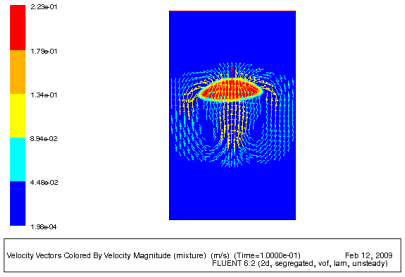

Bubble configurations at a) t = 0.1s, α_s = 0.05 N/m

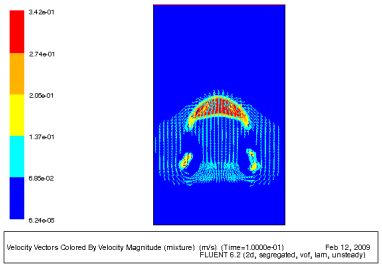

b) t = 0.1s, α_s = 0.005 N/m;

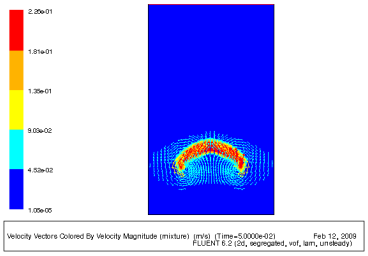

c) time 0.05s, α_s = 0.0005 N/m

Figure 4-4. Rising bubbles attaining different shapes owing to the recirculation zone below them

These results are in perfect harmony with the simulation results of the independent group which was mentioned earlier (3).

4.3. Case 3: Rigid Ellipsoidal Bubble Rising Around an Angular Wall

Domain dimensions are 2 x 2 cm with two angled walls Normal bubble rising problem with constant surface tension specification (0.05 N/m). Surface tension was included to come closer to the case description. Due to surface tension, the bubble tends to attain minimum surface area as the liquid has a phobia towards it. As the surface tension value is quite high in our case, the bubble should not undergo easy break-up.

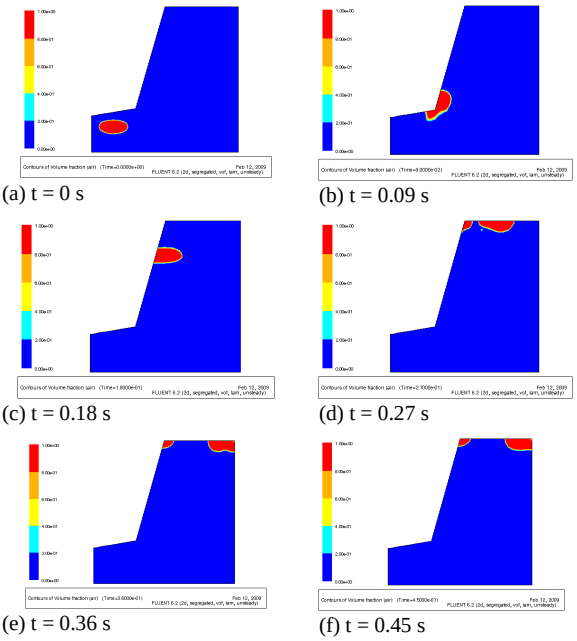

(a) t = 0 s (b) t = 0.09 s

(c) t = 0.18 s (d) t = 0.27 s

(e) t = 0.36 s (f) t = 0.45 s

Figure 4-5. Air bubble position at different times under stronger surface tension effects

The bubble is at different positions compared to the literature values. This must be due to different densities being taken for the liquid phase (our liquid is cryolite). As the surface tension effects are considerable, the bubble tends to avoid contact with the liquid (and rather prefers contact with the wall) while moving up under the action of buoyancy. The following images show the bubble behaviour for weaker surface tension effects of the liquid, where the bubble does not necessarily oppose contact with the liquid while moving up due to buoyancy

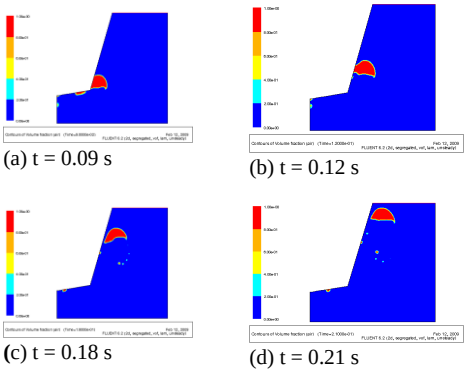

(a) t = 0.09 s (b) t = 0.12 s

(c) t = 0.18 s (d) t = 0.21 s

Figure 4-6. Air bubble position at different times under weaker surface tension effects

4.4. Case 4: Around 20 Bubbles with Random Distribution Rising in a Column

Domain dimensions are 8 cm x 4 cm. 20 numbers of bubbles are taken for the analysis. Analysis is done for 27 time steps

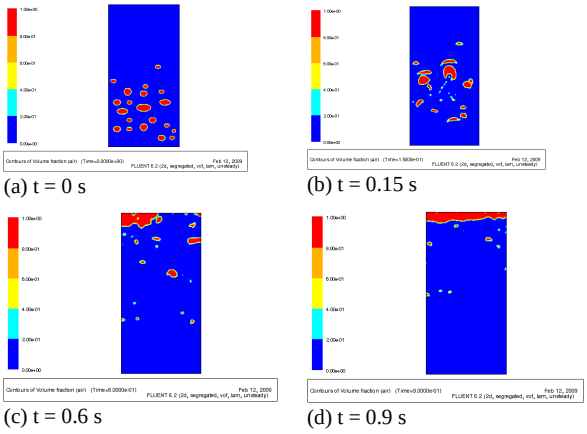

(a) t = 0 s (b) t = 0.15 s

(c) t = 0.6 s (d) t = 0.9 s

Figure 4-7 .Twenty air bubbles coalescing and rising under strong surface tension and buoyancy effect

The results show that the buoyant force acts on all of the bubbles and pushes them upwards. It is also visible that the bubbles below are caught up in the wake of the ones above them and are pulled towards such low pressure areas due to which they end up moving even in a zigzag fashion. The surface tension value being high, results in the bubbles coalescing as the liquid would prefer to minimize the surface contact area with the bubbles. As a result, the number of bubbles reduces drastically and ultimately there is an air column formed in the top region of the column. Some of the small bubbles are caught up in the eddies and tend to remain for relatively longer period within the liquid as they easily give-in to the fluid behavior due to their own lower inertia

5. Conclusion:

Since the results obtained by the VOF multiphase model of FLUENT demonstrate the typical C-shape morphology of the bubbles as they rise up the column (as evident from the animation), the FLUENT results are much more accurate compared to the simplified mathematical model applied in the publication. Multi bubble analysis shows the real effect of bubble in the bottom of the anode plate in soderberg pot. The formed bubbles are collapsed with the aid of increasing the pressure in the feeding of Alumina and prevent the bubbles deposited on the anode surface. Hence, we can obtain the minimum energy consumption and enhance the current efficiency in the soderberg pot.

References

[1] A New Study On Bubble Behavior On Carbon Anode In Aluminum Electrolysis. Gao, Bingliang, et al. [ed.] Halvor Kvande. s.l. : TMS (The Minerals, Metals & Materials Society), Light Metals 2005.

[2] Numerical Simulation Of Bubble Coalescence Using A Volume Of Fluid (Vof) Model. Delnoij, E, Kuipers, J.A.M. and Van Swaaij, W. P. Lyon : s.n., 1998. Third International Conference on Multiphase Flow, ICMF'98.

[3] A New Modelling For Simulating Bubble Motions In A Smelter. Michel, V. Romerio, Alexei, Lozinski and Jacques, Rappaz. [ed.] Halvor Kvande. s.l. : The Minerals, Metals & Materials Society), Light Metals 2005.

[4] B. Glorieux et al., "Density of Superheated and Undercooled Liquid Alumina by a Contactless Method", Int. J. Thermophys., Vol. 20, No. 4, 1999, 1085 – 1094.

[5] T.J.Chung, Computational Fluid Dynamics, Cambridge, UK, Cambridge University Press, 2002.

[6] M.Dupuis, "Computation of Aluminum reduction Cell Energy Balance Using ANSYS® Finite Element Models", TMS Light Metals, 1998, 409 – 417.

[7] M. Dupuis and al., "Cathode Shell Stress Modelling", TMS Light Metals, 1991, 427 – 430.

[8] M. Dupuis, " Computation of Accurate Horizontal Current Density on Metal Pad Using a Full Quarter Cell Thermo-electric Model", CIM Light Metals, 2001, 3-11.

[9] M. Dupuis and I. Tabsh, "Thermo-Electro-Magnetic Modeling of a Hall-Heroult Cell", Proceeding of the ANSYS ® Magnetic Symposium, 1994, 9.3 – 9.13.

[10] M. Segatz and D.Vogelsang, "Effect of Steel Parts on Magnetic Fields in Aluminum Reduction Cells", TMS Light Metals, 1991, 393 – 398.

[11] D.Richard and al., "Thermo-electro-mechanical Modelling of the Contact between Steel and Carbon Cylinders using the Finite Element Method", TMS Light Metals, 2000, 523-528.

[12] I.Eick and D.Vogelsang, "Dimensioning of Cooling Fins for High – Amperage Reduction Cells", TMS Light Metals, 1999, 339 – 345.

[13] C.Vanvoren and al., "AP 50: The Pechiney 500 kA cell", TMS Light Metals, 2001, 221 -226.

[14] H.Kvande and W.Haupin, "Inert Anodes for AI Smelters: Energy Balance and Environmental Impact" JOM, Vol. 53, No. 5, 2001, 29-33.

[15] Bruggeman and D.J.Danka, "Two-Dimensional Thermal Modelling of the Hall-Heroult Cell", Light Metals, 1990, 203-209.

[16] Schmidt-Hatting and al., "Heat Losses of Different Pots". Light Metals, 1985, 609-624.

[17] Antille and al., "Effects of Current Increase of Aluminium Reduction Cells", Light Metals, 1995, 315-321.